CrossMark

Microporous carbon fibers prepared from cellulose as efficient sorbents for removal of chlorinated phenols

Esra Bilgin Simsek[1] · Ivan Novak[2] ·
Ondrej Sausa[3] · Dusan Berek[2]

Abstract Cellulose-based microporous carbon fibers (CFs) were evaluated for the adsorption of 2-Chlorophenol (CP), 2,4-Dichlorophenol (DCP), and 2,4,6-Trichlorophenol (TCP), which are persistent organic pollutants in wastewater. CFs with different surface area values were prepared by using $ZnCl_2$ as a chemical activator, and the samples were characterized by BET, FTIR, SEM, PALS, Zeta potential, and pH titration analysis. The point of zero charge values for CF-1, CF-2, and CF-3 were found as 8.14, 6.79, and 7.01, respectively. The surface area of CFs were determined as 454 m^2/g (CF-1), 760 m^2/g (CF-2), and 1217 m^2/g (CF-3), and PALS measurements at ambient temperature and vacuum indicated the effective pore diameter of about 0.6 nm for all samples. The adsorption of chlorophenols was examined at different solution pH, temperature, and contact time. At the optimum pH of 6.0, the DCP adsorption capacities of CFs, namely, CF-1, CF-2, and CF-3 were calculated as 29.27, 229.81, and 244.09 mg/g, respectively. The adsorption capacity of the CF-3 sample was found to be an ideal adsorbent for CPs removal from aqueous solutions. A comparison of the adsorption kinetic data was best described by the pseudo second-order and particle diffusion models. For the CF-2 sample, the initial sorption rates of CP, DCP, and TCP were found in the increasing order as 2.084, 32.23, and 43.63 mg/g min. Similar order of the sorption rates were also observed for CF-1 and CF-3 samples. The obtained results demonstrated the fact that among the CP homologues, TCP showed both a higher affinity and a higher diffusion rate for all CFs. The adsorption process was found to be exothermic, and

✉ Esra Bilgin Simsek
esrabilgin622@gmail.com; ebilgin.simsek@yalova.edu.tr

[1] Chemical and Process Engineering Department, Yalova University, 77100 Yalova, Turkey

[2] Polymer Institute, Slovak Academy of Sciences, 84541 Bratislava, Slovakia

[3] Institute of Physics, Slovak Academy of Sciences, 84511 Bratislava, Slovakia

the entropy values were positive, depicting that CPs were randomly distributed at the solid/solution interface.

Introduction

Chlorinated phenols (CPs) constitute an important group of phenolic contaminants, which have one or more chlorine atoms in their structures [1]. Due to their high toxicity, strong odor emission, low biodegradation and accumulation in live organisms chlorophenols are classified as hazardous substances in the environment [2, 3]. Some of their isomers may act also as promotors or cocarcinogens, and the human immune system is likely sensitive to their toxic effects. They are directly employed as pesticides, herbicides, wood and leather preservatives, fungicides, and disinfectants and are also created by the decomposition of some more complex chemicals used in agriculture [4]. CPs can be detected in soil, groundwater, and even in the food chains [3]. Chlorophenols are also produced in the effluent streams discharged by petroleum refining processes, coal tar from gasification and liquefaction, production of steel, dyestuff and paper, as well as by textile and leather industries [5]. Furthermore, lower chlorinated phenols may also be present during the treatment of water with chlorine in the presence of certain other contaminants. Hence, due to their harmfulness to humans and also animals [6], chlorophenolic compounds should be eliminated from the environment, especially from drinking water.

To date several approaches including photocatalytic and oxidative degradation, and adsorption have been reported for removal of CPs from different sources [1]. Adsorption is a widely used technique for water decontamination [7, 8] and is successfully performed for the removal of CPs using carbon allotropes, i.e., activated carbon [9, 10], carbon fibers [11–14], carbon nanotubes [15–17], and graphene [1]. The porous carbon materials with large pore volume, high surface area, and regular pore size are good candidates as efficient adsorbents with high adsorption capacities [18–20].

Carbon fibers (CFs) have unique narrow pore size distribution with large surface area where the micropores are directly exposed on the carbon surface [14]. The adsorption energy is increased within narrow-size pores [12], and the large surface is expected to increase sorption capacity of the material. These surface features of CFs make them ideal to be used as highly efficient adsorbents instead of other carbon-based materials. Wang et al. [11] examined the activated carbon fibers activated by static air (surface area of 702 m^2/g) and examined the adsorption of 2,4-dichlorophenol (DCP). Lu and Sorial [14] investigated the activated carbon and carbon fibers with different pore size distribution for the adsorption of phenolic compounds. They found that the smallest critical pore size and narrow pore size distribution were more efficient in hampering oligomerization of phenolics in binary sorption systems. Liu et al. [12] studied the impact of the substituent groups of

phenols onto the adsorption performance of commercial ACFs. They found that ACFs show a high adsorption rate due to their open pore structure, and steric effects played an important role in the kinetics of some CPs having wide molecular dimensions owing to the restriction of the pore structure and the retardation of the adsorbed molecules.

However, to the best of our knowledge, little information is available concerning the comparison of chlorophenol adsorption performances of CFs with different surface areas. Herein, the purpose of our study was to examine and compare the adsorptive properties of novel CFs prepared by the simple and economic method of cellulose carbonization. The basic physical properties of CFs were studied, and the effects of experimental parameters such as contact time, solution pH, adsorbent dosage, and temperature on the CP adsorption were investigated. Equilibrium data were applied to isotherm models; and thermodynamic and kinetic parameters were used to identify the possible adsorption mechanism.

Materials and methods

Chemicals and reagents

Samples of microporous carbon were prepared from microfibers of delignified cellulose Greencel (Pulp factory, Hencovce, Slovakia). The 2-Chlorophenol (2-CP), 2,4-dichlorophenol (2,4-DCP), and 2,4,6-trichlorophenol (2,4,6-TCP) were purchased from Sigma Aldrich. All the chemicals used in the experiments were of analytical reagent grade. Milli-Q water was used throughout this study.

Preparation of carbon fibers

CF-1

The 100 g of cellulose microfibers was placed into a stainless steel vessel provided with a tightly sealed lid and carbonized in an oven at 700 °C for 1 h in a protective atmosphere of carbon dioxide formed in the first stage of carbonization.

The effect of increased surface area was tested with samples prepared by chemical activation. The activation was primarily directed toward liberation of micropores likely occluded by tar formed during carbonization. As a result release of volatile products was facilitated and the number of pores increased. Zinc dichloride was employed as chemical activator.

CF-2

The 100 mL of zinc dichloride solution (15 wt%) was added to 20 g of cellulose microfibers and the mixture was thoroughly stirred. A thin layer of the resulting slurry was dried at 120 °C and carbonized for 1 h as in the case of CF-1 preparation, however, at 600 °C. Resulting carbon fibers were carefully washed with distilled water to remove $ZnCl_2$ and dried for 12 h at 80 °C.

CF-3

The 100 mL of zinc dichloride solution (30 wt%) was added to 20 g of cellulose microfibers and stirred. The subsequent procedures were identical to those of CF-2 preparation.

Characterization techniques

Potentiometric titration data were measured by the method described by Helfferich [21]. The electrophoretic mobilities of CFs were analyzed using a Malvern Instruments Zetasizer 3000HSA. Chemical structure of CFs was assessed with the help of a Fourier transform infrared (FTIR) spectrophotometer (Perkin Elmer Spectrum One) using attenuated the total reflectance method. The morphology of carbon fibers was examined using a Philips XL30 ESEM-FEG/EDAX system. Surface area of the carbon fibers was calculated from adsorption isotherms of argon at 77 K determined on a home-made glass apparatus. Positron annihilation lifetime spectroscopy (PALS) was done with the help of a conventional fast–fast coincidence spectrometer. The instrumental resolution function as well as source correction was determined by defect-free Al samples. The positron lifetime spectra were analyzed by the PATFIT-88 software package [22]. If the bound state of electron and positron, namely positronium (commonly used as a probe for the free volume determination) is not created in the investigated material, then the effective void size can be estimated from the second component of lifetime spectra by the approach of Liao et al. [23] using the equation:

$$\tau_2 = 0.260 \times [1 - R/(R + 0.3823) + (1/2\pi) \times \sin(2R/(R + 0.3823))]^{-1}, \quad (1)$$

here τ_2 is positron lifetime in nanoseconds and R is free-volume radius in nm (spherical approximation of void shape). Formula is valid up to about 1 nm effective pore diameter. The relative intensity of the second component can be attributed to a number of free volume voids in the investigated carbon fibers.

Adsorption experiments

Batch sorption experiments were carried out with 25 mL of the chlorophenol solution with initial concentration of 50 mg/L at measured pHs of 5.90, 6.16, and 4.99 for CP, DCP, and TCP, respectively. Adsorption isotherms were applied by varying the amount of adsorbent at laboratory temperature (±24 °C). Equilibrium concentrations before and after adsorption were analyzed using a UV–Vis spectrophotometer (SHIMADZU UV1800) at 273, 285, and 290 nm wavelengths, respectively. Each experiment was duplicated under identical conditions and the average results were reported. The uptake of chlorophenol at equilibrium was calculated as:

$$q_e = \frac{(C_i - C_e) \times V}{m}, \quad (2)$$

where q_e is the sorption capacity (mg/g), V is the volume of solution (L), m is the adsorbent dosage (g), C_i and C_e are the initial and equilibrium concentrations (mg/L), respectively.

The effect of pH on the adsorption of CPs was examined by varying the solution pH from 2.0 to 10.0 using HCl or NaOH solution with appropriate concentration.

The kinetic experiments were conducted by mixing the defined amount of each CF with 50 mg/L CP solution in a polyethylene bottle by using a water bath temperature controlled shaker (WITEG SHO 2D) at 25 °C. Adsorbent dosage for CF-1 and CF-2 and CF-3 samples was selected as 4 and 0.2 g/L, respectively.

Results and discussion

Characterization results

Figure 1 shows the FTIR spectra of CF-1, CF-2, and CF-3 before and after CP adsorption. General bands at 2390, 2080, 1860, 1560, and 1140 cm^{-1} appeared at the FTIR spectrum of all CFs. The absorption bands at 1560 cm^{-1} can be assigned to the aromatic C=C stretching vibrations [24]; where the C–O band was centered at 1140 cm^{-1} due to the C−O stretching [25]. The peaks at 1860 cm^{-1} corresponded to C=O stretching, and the bands at 2080–2390 cm^{-1} are assigned to the C–H bonds. For CF-2 and CF-3 samples, a decrease in the intensities of the asymmetric and symmetric C–H stretching bonds could be related to the action of the zinc chloride as a dehydrating agent [26] or decomposition of cellulose, hemicellulose, and lignin by activation. Following removal of CPs by CFs, the new peaks occurred at about 1360 and 1200 cm^{-1}. The band at 1360 cm^{-1} corresponds to the C–O [27] or C=C stretching vibration [28] while the peaks at 1206 cm^{-1} pertain to phenolic structures [24, 29].

PALS measurements performed at both ambient temperature and vacuum show the effective free volume radius of about 0.32 nm for all samples. This average value was determined from the second component of lifetime spectra by equation (Eq. 1). Positronium is not created in our pristine carbon fibers. However relative intensity of the second component, which reflects the number of the free volume voids increases with the surface area of samples (Fig. 2).

The surface charge of carbonaceous adsorbents depends on the solution pH and their PZC values; the carbon fiber surface is positively charged at pH < pH$_{PZC}$, while it is negatively charged at pH > pH$_{PZC}$. The proton binding and zeta potential (ξ) profiles of CFs are presented in Fig. 3. The pH$_{PZC}$ for CF-1, CF-2 and CF-3 were determined as 8.14, 6.79, and 7.01, respectively. The pH$_{IEP}$ values were found to be 4.3, 6.7, and 6.9, respectively.

In order to examine the morphological features and surface characteristics of the CFs, SEM micrographs (1000× and 5000× magnification) of CFs were obtained and are compared in Fig. 4. The surface structure of the samples proved that the fibers were arranged in a random way, and had a shape with longitudinal and smooth fibrous texture. When compared with the CF-1 sample, CF-2 and CF-3
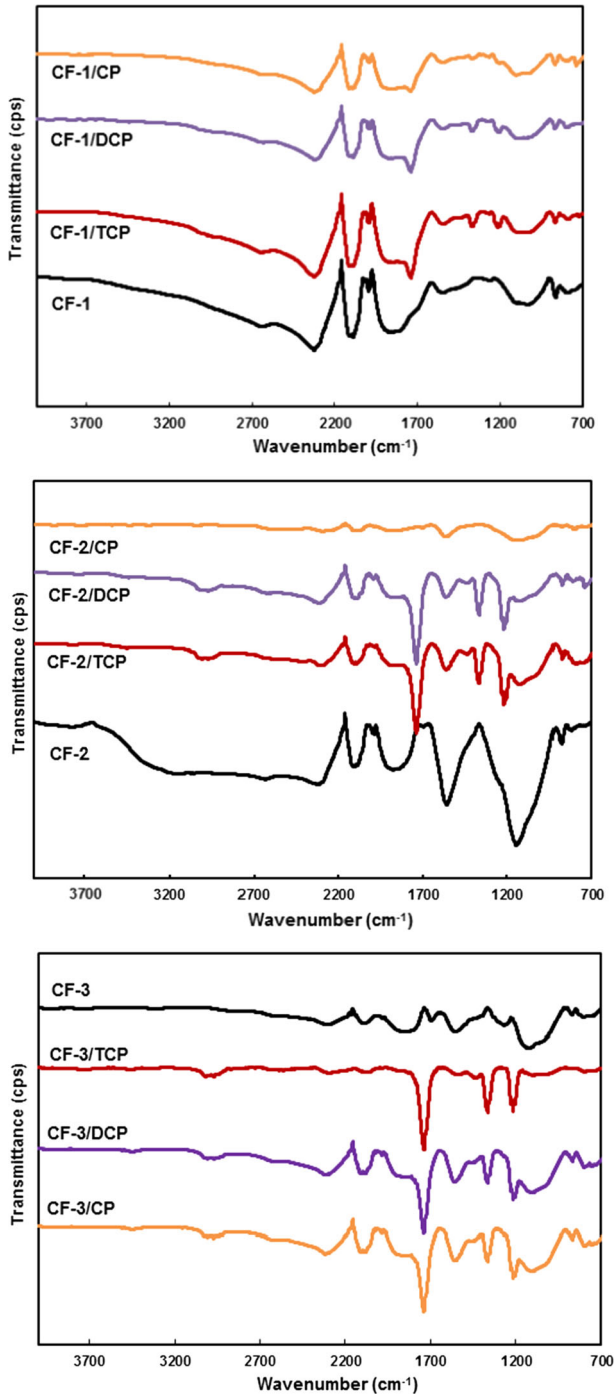
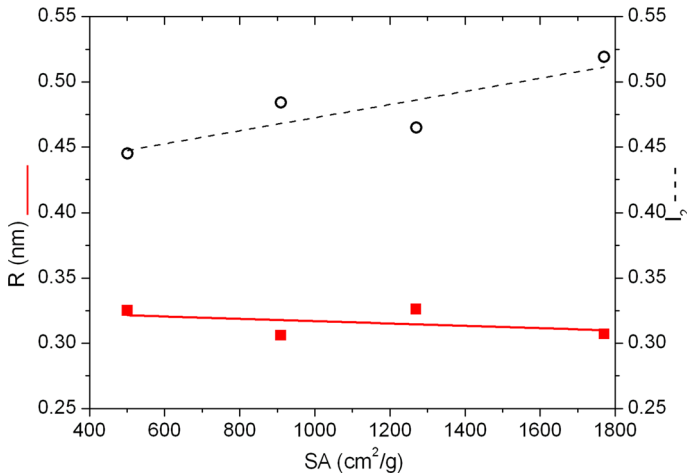**Fig. 1** FTIR spectra of CFs before and after CP adsorption

Fig. 2 Influence of surface area (SA) on free volume hole size (R) and number of free volume voids (I_2) in CF samples

carbon fibers exhibited similar structure indicating that the modifier addition had no effect on the shape except for the surface area.

Equilibrium studies

Effect of solution pH

As the solution pH mainly influences the adsorption, experiments were conducted at different pHs and the results are presented in Fig. 5. The pK_a values of TCP, DCP, and CP are 6.7, 7.4, and 8.4, respectively. As can be seen in Fig. 5, chlorophenol removal is slightly increased at pH $< pK_a$ for each phenol, except for a slight decrease at pH 2.0, according to the decreased interactions between protons on the basic sites and the phenols. The pH_{PZC} of CFs were found between pH 7.0 and 8.0 and when pH $> pK_a$, electrostatic repulsion occurs between the dissociated phenols and the negatively charged surface. Additionally, the dissociation of phenols leads to a decrease in the hydrophobicity, following decreased affinity between chlorophenols and the CFs surface [12]. As the optimum pH for CPs removal was found at pH 6.0, subsequent experiments were conducted at the original pH values of CPs (pH 6.0–7.0).

At the optimum pH of 6.0, the DCP adsorption capacities of the carbon fiber samples of CF-1, CF-2, and CF-3 were calculated as 29.27, 229.81, and 244.09 mg/g, respectively. The specific surface area of CF-1 (454 m^2/g) increased significantly for CF-2 (760 m^2/g) and CF-3 (1217 m^2/g) samples, and in parallel the uptake capacity increased notably between these samples demonstrating the fact that the specific surface area plays a critical role in the uptake capacity. Analogous results were also observed for CP and TCP adsorbates.
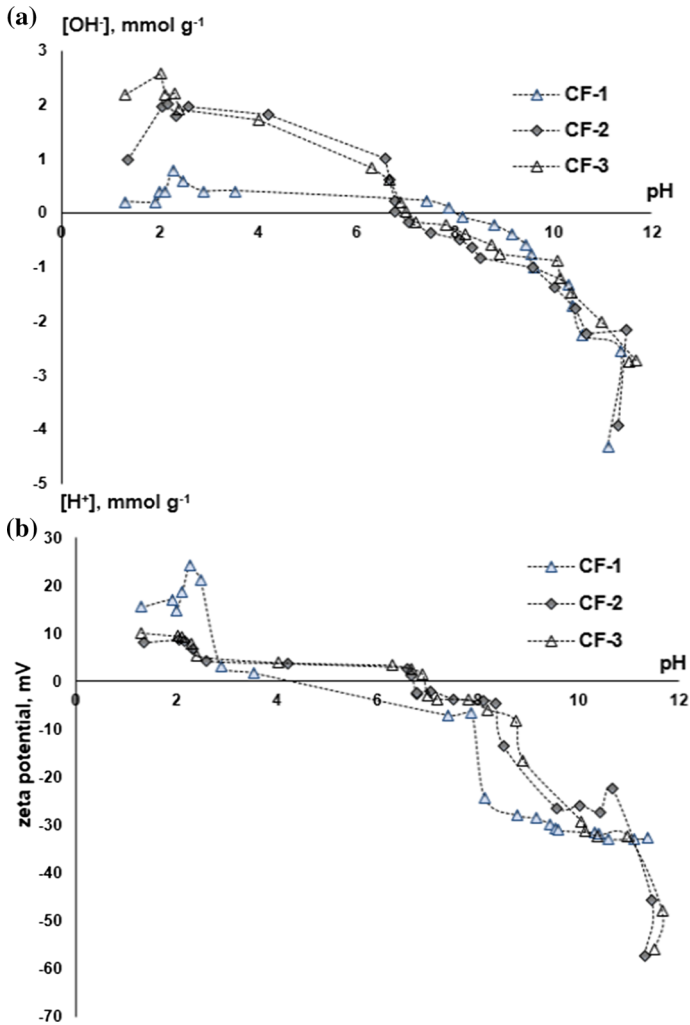
Fig. 3 Proton binding curves (a) and Zeta potential measurements (b) of CFs

On the other hand, chlorophenol uptake increased with the increasing number of the chlorine group. At pH 6.0, the CP, DCP, and TCP uptake capacities of the CF-2 sample were found to be 95.32, 229.8, and 258.8 mg/g, respectively (Fig. 6). Phenol adsorption onto the carbonaceous adsorbents was mostly controlled by the synergetic effects of the π–π interaction and electrostatic attraction with the former dominant at pH $< pK_a$ [16]. The π–π interaction derives from the interactions between the π electrons in the aromatic rings and carbon surface. CFs are expected to work as an electron donor, and the benzene ring with chlorine substituent acts as an electron withdrawing group [30]. When the number of electron withdrawing
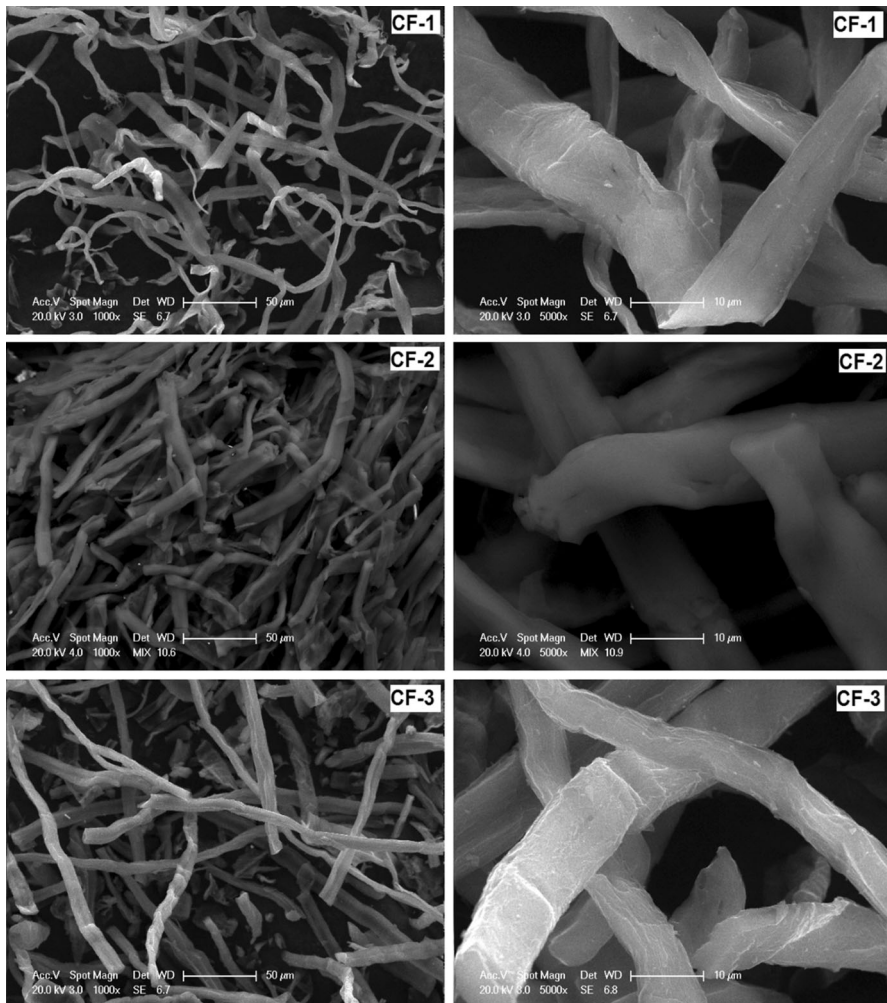
Fig. 4 SEM images of CFs

groups increased, the electron density in the aromatic ring decreased, and; therefore, TCP has the highest affinity to the π electrons in the carbon fiber surface.

Adsorption isotherms

The equilibrium characteristics of chlorophenol adsorption onto the CFs were examined by the Freundlich, Langmui,r and Dubinin–Radushkevich isotherm models. The parameters of isotherm models and their correlation coefficients (R^2) are presented in Table 1. It could be seen that the Freundlich and Dubinin–Raduskevich models with the greater correlation coefficients ($R^2 > 0.91$) were more suitable for describing the adsorption of chlorophenols onto the carbon fibers.
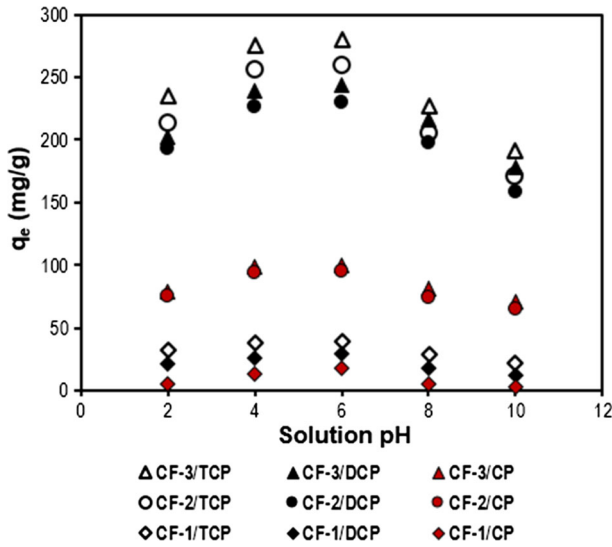
Fig. 5 Effect of solution pH on CFs

According to the model adsorption capacities (i.e., K_F, Q), the order of carbon fibers was found as CF-3 > CF-2 > CF-1, and for the sequence concerning phenols, it was TCP > DCP > CP. The Freundlich isotherm model is the most widely employed empirical model based on the surface heterogeneity, exponential distribution of active surface sites, and their energies toward adsorbate [16]. The unique chemical structure of carbon fibers possessed outstanding thermal and chemical stability, so as seen in Fig. 7, the Freundlich isotherm fitted well. Table 2 represents the Freundlich isotherm constants for CPs adsorption onto carbonaceous adsorbents reported in the literature.

Kinetic studies

The adsorption kinetics are an essential index to evaluating the efficiency of adsorption. In the current work, the kinetics of the CPs adsorption data were analyzed with the pseudo-first-order, the pseudo-second-order model, and the Weber–Morris intra-particle diffusion model.

The pseudo-first order equation is usually applied for the adsorption on liquid/solid surfaces [31] and it is formulated as:

$$\log(q_e - q_t) = \log(q_e) - \left(\frac{k_1}{2.303}\right) \cdot t, \tag{3}$$

where q_t is the adsorbed amount at time t and k_1 is the sorption rate constant (min^{-1}).

The pseudo-second order model rate expression [32] is given by the following equation:

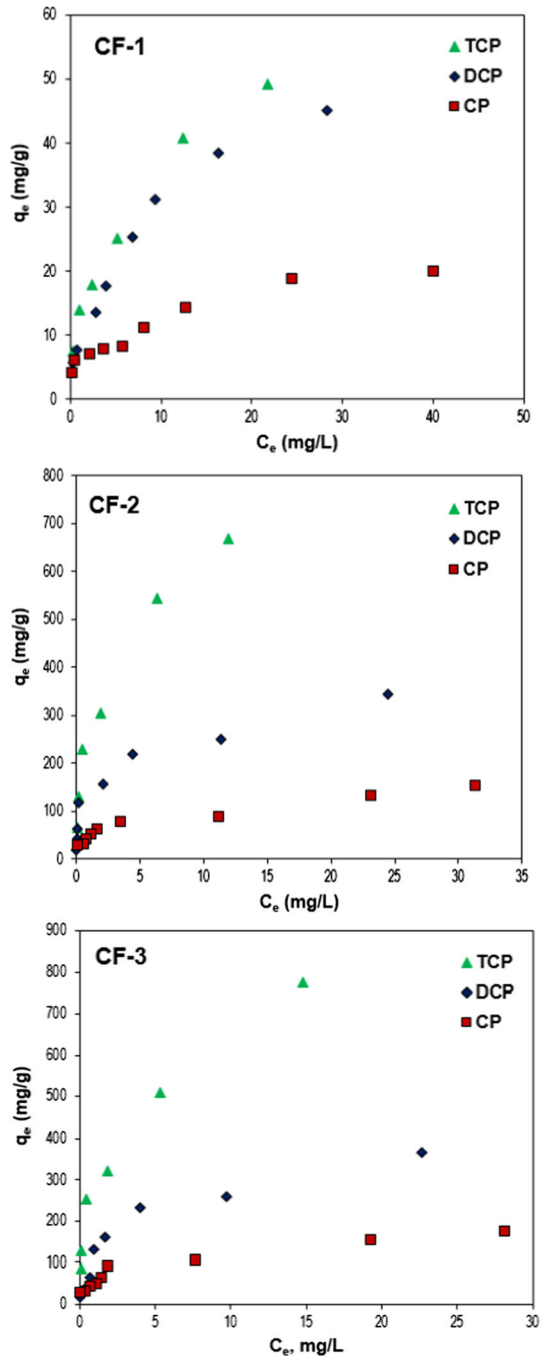**Fig. 6** Comparison of CP adsorption capacities of CFs

Table 1 Adsorption isotherm constants of CFs

Adsorbent	Langmuir			Freundlich			Dubinin–Raduskevich			
	Q (mg/g)	b	R^2	K_F [mg/g(L/mg)$^{1/n}$]	$1/n$	R^2	Q (mmol/g)	β	E (kJ/mol)	R^2
CP										
CF-1	12.09	1.404	0.830	5.69	0.328	0.939	0.380	2.5E−09	14.111	0.916
CF-2	80.361	2.031	0.735	44.22	0.344	0.962	3.267	2.6E−09	13.807	0.958
CF-3	79.867	3.44	0.660	51.24	0.367	0.947	4.154	2.7E−09	13.568	0.957
DCP										
CF-1	26.87	0.815	0.888	9.44	0.486	0.986	1.431	3.5E−09	11.791	0.978
CF-2	246.37	2.960	0.934	124.49	0.306	0.976	3.988	1.7E−09	16.713	0.984
CF-3	160.96	2.194	0.759	96.38	0.483	0.912	5.557	2.3E−09	14.584	0.922
TCP										
CF-1	32.76	0.916	0.944	12.71	0.443	0.996	1.231	3.2E−09	12.486	0.992
CF-2	611.91	1.231	0.972	240.71	0.444	0.982	20.004	3.0E−09	12.903	0.981
CF-3	584.52	1.736	0.945	269.07	0.401	0.948	17.226	2.7E−09	13.562	0.955

Fig. 7 Comparison of Freundlich and experimental adsorption capacities of CFs
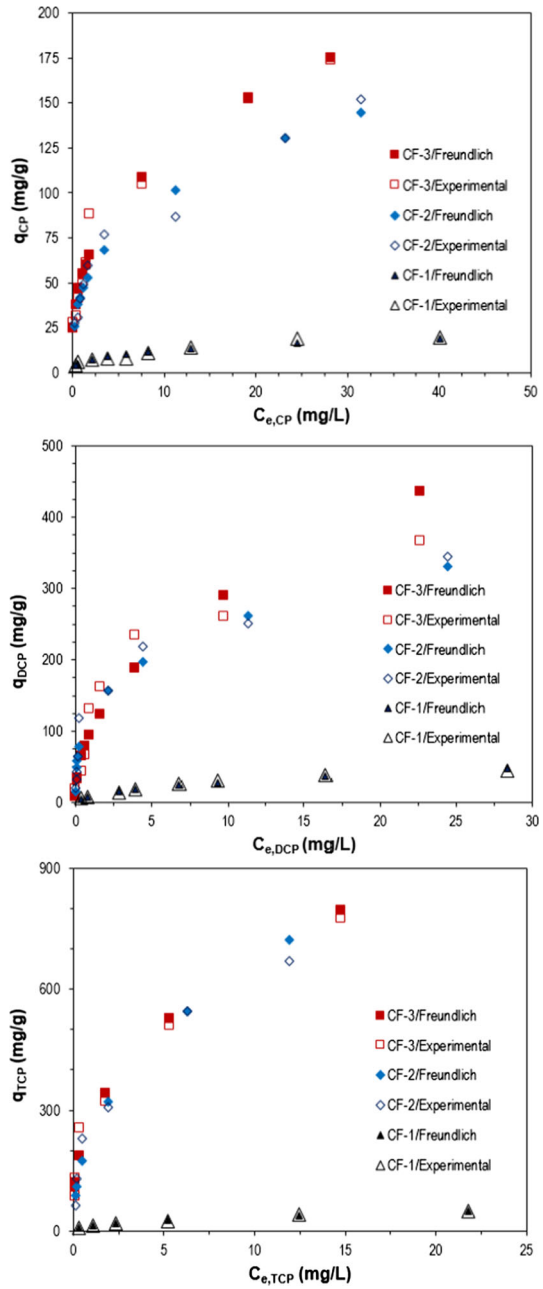
Table 2 Comparison of Freundlich isotherm constants for CPs adsorption onto carbonaceous adsorbents

CP	Adsorbent	Surface area (m²/g)	K_F [mg/g (L/mg)$^{1/n}$]	Reference
2-CP	Surface functionalized single-walled carbon nanotube	625	24.95	[15]
	Low-cost coir pith carbon	167	12.8	[34]
	Activated carbon			
	SA4	800	86.5	[35]
	CA1	1400	13.6	[35]
	PKDA	850	60.4	[35]
	CAgran	1400	8.2	[35]
	Pitch-based activated carbon fiber	920.3	285.7	[12]
	Carbon fiber-I	454	5.69	This study
	Carbon fiber-II	760	44.22	This study
	Carbon fiber-III	1217	51.24	This study
2,4-DCP	Activated carbon fiber activated by static air	702	55.1	[11]
	Surface functionalized single-walled carbon nanotube	625	54.85	[15]
	Multi-Walled carbon nanotube [MWCNT/ 60–100 nm)]	40–70	4.155	[16]
	Pitch-based activated carbon fiber	920.3	432.6	[12]
	Maize cob carbon	468	17.94	[9]
	Carbon fiber-I	454	9.4	This study
	Carbon fiber-II	760	124.49	This study
	Carbon fiber-III	1217	96.38	This study
2,4,6-TCP	Surface functionalized single-walled carbon nanotube	625	122.9	[15]
	Pitch-based activated carbon fiber	920.3	541.2	[12]
	Activated carbon derived from oil palm empty fruit bunch	N.I.[a]	22.04	[36]
	Carbon fiber-I	454	12.71	This study
	Carbon fiber-II	760	240.71	This study
	Carbon fiber-III	1217	269.07	This study

[a] Not indicated

$$\frac{t}{q_t} = \frac{1}{k_2 \cdot q_e^2} + \frac{1}{q_e} t, \tag{4}$$

where k_2 is the rate constant (g/mg min). The q_e and k_2 values are obtained from the slope and intercept of the plot t/q_t against t. Initial adsorption rate (h, mg/g min) can be determined according to the Eq. (5):

$$h = k_2 q_e^2. \tag{5}$$

Table 3 shows the correlation coefficients and the rate constants of the pseudo-first and pseudo-second-order models. The first-order model showed poor fitting

Table 3 Comparison of kinetic models for CPs adsorption onto CFs ($T = 25$ °C)

Adsorbent	CF-1			CF-2			CF-2		
CP	CP	DCP	TCP	CP	DCP	TCP	CP	DCP	TCP
q_e (mg/g)	8.190	10.292	12.587	90.62	160.76	214.17	186.85	232.31	264.26
Pseudo-first order									
q_e (mg/g)	3.883	4.641	4.304	63.64	46.10	59.95	147.04	74.66	62.91
k_1 (1/min)	0.014	0.020	0.029	0.014	0.033	0.031	0.022	0.031	0.031
R^2	0.912	0.841	0.901	0.936	0.901	0.884	0.954	0.901	0.880
Pseudo-second order									
q_e (mg/g)	8.039	10.310	12.727	96.05	162.20	215.91	208.22	234.52	265.81
k_2 ($\times 10^{-2}$ g/mg min)	0.983	1.023	1.300	0.022	0.122	0.193	0.010	0.070	0.092
h (mg/g min)	0.635	1.087	2.107	2.084	32.23	43.63	4.358	39.01	65.12
R^2	0.994	0.998	0.999	0.976	0.999	0.999	0.982	0.999	0.999
Weber–Morris diffusion model									
k_{id-1} (mg/g min$^{0.5}$)	0.461	0.662	0.776	8.247	14.07	20.14	26.68	21.62	20.45
R^2	0.918	0.913	0.963	0.875	0.900	0.899	0.934	0.917	0.852
k_{id-2} (mg/g min$^{0.5}$)	0.150	0.073	0.030	3.896	1.953	2.267	7.630	3.364	2.711
R^2	0.971	0.888	0.989	0.995	0.969	0.982	0.987	0.967	0.951

with low R^2 values and remarkable differences between the experimental and theoretical adsorption capacities were observed. On the other hand, the second-order model exhibited higher correlation coefficients ($R^2 > 0.99$) for all chlorophenols. The experimental and theoretical capacities of this model were found to be very close, indicating that it was more suitable for defining the adsorption progress of CPs onto CFs. Moreover, the second-order rate index, k_2 values of carbon fiber samples follow the order of CF-1 < CF-2 < CF-3 for all phenols.

Considering the pseudo-second equation, the TCP removal performance was found much higher when compared with CP and DCP for all carbon fibers. The TCP rate constant (k_2) was greater than that of CP and DCP demonstrating that the diffusion rate into the pores was higher. This result can be ascribed to the higher acidity of the tri- and di-chlorophenols [10].

On the other hand, for the CF-2 sample, the initial sorption rates (h) of CP, DCP, and TCP were found in the increasing order as 2.084, 32.23, and 43.63 mg/g min. Similar phenomena have also been observed for CF-1 and CF-3 samples, which indicated higher affinity of TCP.

The Weber–Morris particle diffusion model is defined as:

$$q_t = k_{id}t^{0.5} + C, \qquad (6)$$

where k_{id} (mg/g min$^{0.5}$) is the rate constant; I and C are the number of each sorption stage, and the intercept related with the thickness of boundary layer, respectively
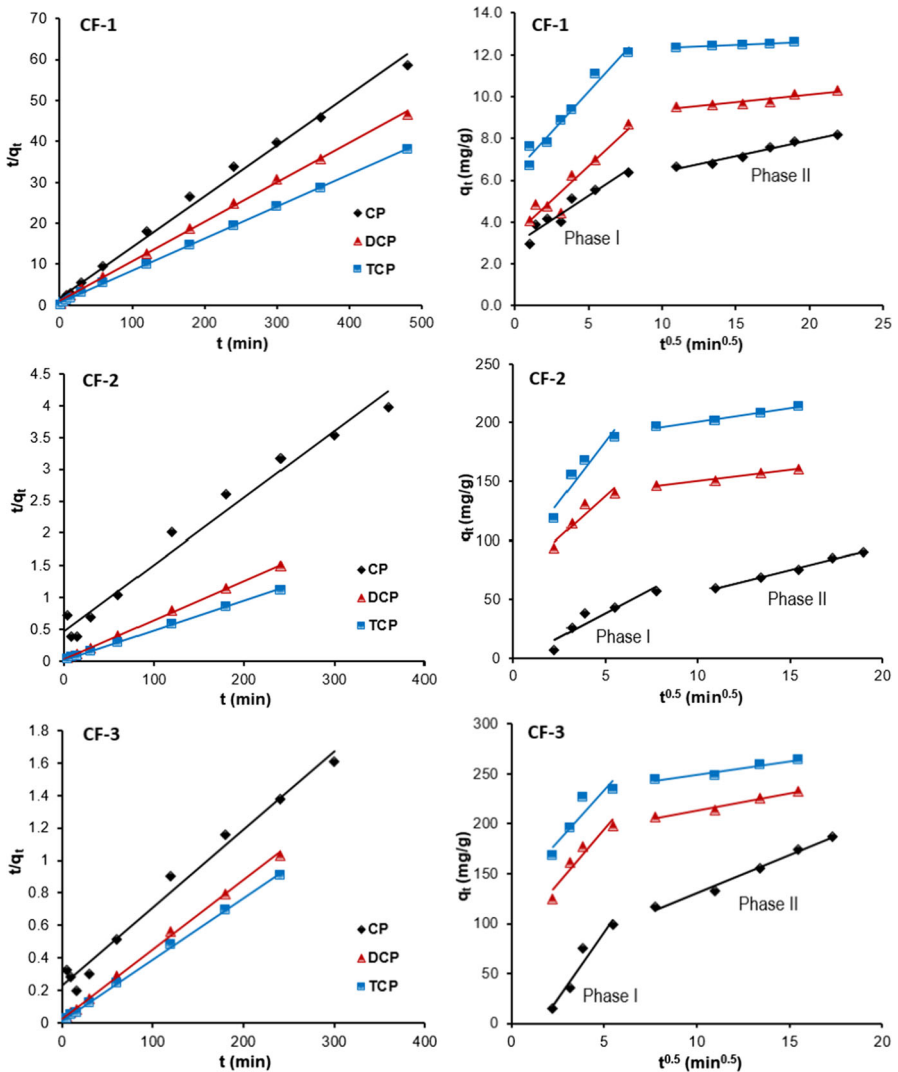
Fig. 8 Pseudo-second order and Weber–Morris diffusion kinetic modelling of CFs

[33]. If the plot of q_t versus $t^{0.5}$ is linear and passes through the origin, the sorption is fitted to the particle diffusion model or else other processes, such as film diffusion, play a role in the sorption system.

Weber–Morris diffusion model parameters including k_{id-1}, k_{id-2}, and R^2 are shown in Table 3, and the fitting plots are demonstrated in Fig. 8. In general, the R^2 values of the second stage were higher than the first stage implying the external mass transfer. The results suggested that the intra–particle diffusion could be the rate-limiting stage in the removal steps.

Adsorption thermodynamics

The effect of temperature on chlorophenol adsorption onto the CFs was deduced from the results of adsorption experiments performed at 25, 35, and 45 °C. The thermodynamic parameters including changes in the standard enthalpy (ΔH°), the Gibbs free energy (ΔG°), and the standard entropy (ΔS°) were calculated using the following equations:

$$\ln K_C = \frac{\Delta S^{\circ}}{R} - \frac{\Delta H^{\circ}}{RT}, \tag{7}$$

where K_c (L mg^{-1}) is the equilibrium adsorption constant [$K_C = ((C_i - C_e) \cdot V)/(C_e \cdot m)$]. The values of ΔH° and ΔS° can be obtained from the slope and intercept of a plot of ln K_C against 1/T. ΔG° can then be calculated using the relation below:

$$\Delta G^{\circ} = -RT \ln K_C. \tag{8}$$

The obtained results are listed in Table 4. The negative values of ΔH° confirmed that adsorption was more efficient at lower temperatures, while negative ΔG° indicated spontaneity of the adsorption process. Positive ΔS° values demonstrated a more disordered structure of the adsorbate at the solid/solution interface. Liu et al. [12] stated that the ΔS° value is related to the displacement of the water molecules adsorbed on the surface. In the present work, for each carbon fiber sample, the ΔS° values increased with the increasing number of chlorine group indicating that water molecules are more adsorbed with higher substitution degrees.

Adsorption mechanism

The phenol adsorption process onto the carbon fibers can be explained with three steps such as: (1) film diffusion including the movement of CP molecules from the bulk solution toward the external CF surface, (2) particle diffusion, where the CP

Table 4 Thermodynamic parameters for the adsorption of CPs onto CFs

	Adsorbent	E_a (kJ/mol)	ΔH° (kJ/mol)	ΔS° (J/mol K)	ΔG° (kJ/mol)		
					298 K	318 K	338 K
CP	CF-1	−6.55	−18.28	15.30	−22.84	−23.15	−23.46
	CF-2	−21.68	−8.93	59.33	−26.61	−27.80	−28.99
	CF-3	−31.48	−18.10	31.88	−27.60	−28.24	−28.87
DCP	CF-1	−5.04	−3.93	57.82	−21.17	−22.32	−23.48
	CF-2	−4.11	−13.68	65.92	−33.32	−34.64	−35.96
	CF-3	−5.44	−12.92	61.90	−31.37	−32.61	−33.85
TCP	CF-1	−8.78	−5.53	60.75	−23.64	−24.85	−26.07
	CF-2	−7.74	−12.62	68.10	−32.92	−34.28	−35.64
	CF-3	−1.99	−7.67	88.54	−34.06	−35.83	−37.60

molecules moved inside of CFs, and (3) adsorption progress, adsorptive attachment of the CP molecules inside a microporous structure [16]. According to the kinetic modeling results, the adsorption rate of chlorophenols was probably controlled by the particle diffusion. The reduced surface area [from 1217 m^2/g (CF-3) to 454 m^2/g (CF-1)] might be also responsible for the adsorption capacity reduction to chlorophenols suggesting that the adsorption was controlled by the inner surface of the CFs. Moreover, the π–π interactions between the carbonaceous surface and the organic pollutant and the chlorine substitution could also affect the sorption mechanism [30].

Regeneration of the exhausted carbon fiber

As the regeneration and reusability of the used carbon make the treatment process economical and also help understand the sorption mechanism, the exhausted CF-3 sample was subjected to desorption tests. Suitable amounts of CF-3 were added to bottles containing 50 mg/L CP concentration, and regeneration was then tested by using NaOH (1 M), ethanol, and methanol as desorption agents. Figure 9a shows the
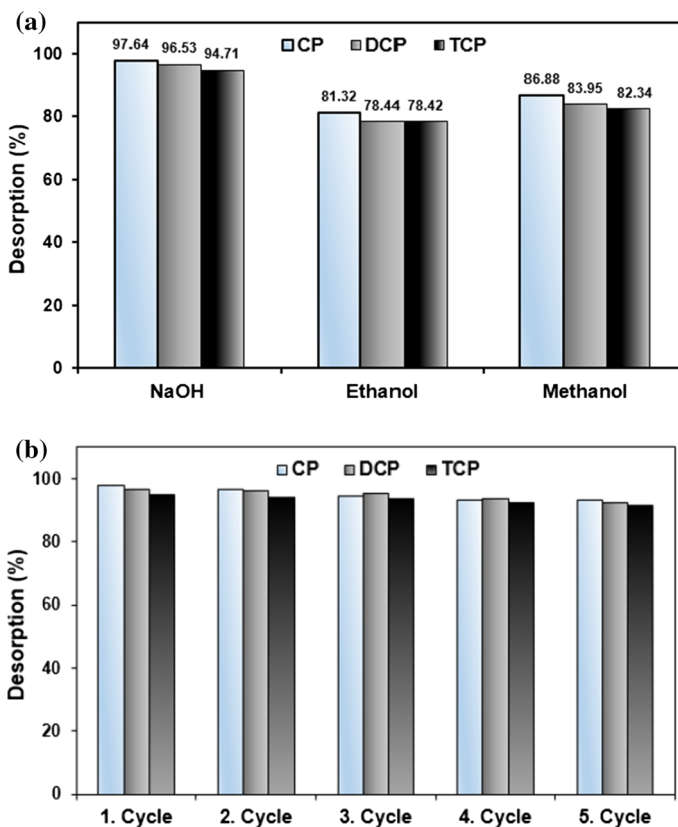

Fig. 9 Desorption efficiencies for different regenerants (**a**) and performance change for each cycle by using NaOH as regenerant (**b**)

CP desorption efficiencies for different chemicals. The DCP desorption efficiencies were found to be 96.5, 78.4, and 83.9 % when NaOH, ethanol, and methanol were used as agents, respectively. Similar results were obtained for other CP homologues. In the literature, attempts were made to desorb phenolic compounds from the used carbons with help of NaOH, ethanol, and methanol [36–39].

After selecting the optimum desorption agent (NaOH), in order to demonstrate the reusability of the sorbent based on microporous carbon fibers, the sorption–washing–drying–desorption–washing–drying cycle was repeated five times, and the results are represented in Fig. 9b. In the first cycle, the TCP desorption efficiency was found to be 94.2 %, while it decreased to 91.5 % after the fifth cycle. In addition, no significant change was observed in the adsorption capacity of CF-3 during the regeneration cycles.

Conclusions

Microporous carbon fibers, CF, were prepared by controlled carbonization of a cellulosic precursor. Their specific surface areas were 454, 760, and 1217 m^2/g—designated CF-1, CF-2, and CF-3, respectively. Scanning electron microscopy revealed that the fibers had macroscopically smooth textures. The sorption of chlorinated phenols from a water solution on CF was studied in detail. The specific surface area was found to notably influence the adsorptive characteristics of CFs. The excellent adsorption capacities of chlorinated phenols on CFs were observed in the series CF-3 > CF-2 > CF-1. The performed kinetic studies suggested that the adsorption could be well described with the pseudo second-order and particle diffusion models. The adsorption process was found to be exothermic, and the change in entropy was positive, which indicated that the adsorption of the chlorinated phenols on carbon fibers increased the randomness at the solid/solution interface. Considering both the adsorption isotherms and the pH effect, multiple factors such as π–π interactions, as well as electrostatic and hydrophobic interactions were proposed to play an important role on the adsorption of chlorinated phenols on CFs. The current study suggests the large potential for utilization of CFs as effective adsorbents for removal of chlorophenol-based pollutants from an aquatic environment.

References

1. R.A.K. Rao, S. Singh, B.R. Singh, W. Khan, A.H. Naqvi, J. Environ. Chem. Eng. **2**, 199–210 (2014)
2. K.P. Singh, S. Gupta, P. Ojha, P. Rai, Environ. Sci. Pollut. Res. **20**, 2271–2287 (2013)
3. Q. Wen, T. Yang, S. Wang, Y. Chen, L. Cong, Y. Qu, J. Hazard. Mater. **244–245**, 743–749 (2013)
4. A. Bhatnagar, A.K. Minocha, E. Kumar, M. Sillanpää, B.-H. Jeon, Sep. Sci. Technol. **44**, 3150–3169 (2009)
5. N. Khanikar, K.G. Bhattacharyya, Chem. Eng. J. **233**, 88–97 (2013)
6. A. Mittal, D. Kaur, A. Malviya, J. Mittal, V.K. Gupta, J. Colloid Interface Sci. **337**, 345–354 (2009)
7. T.A. Saleh, V.K. Gupta, Environ. Sci. Pollut. Res. **19**, 1224–1228 (2012)
8. V.K. Gupta, S. Agarwal, T.A. Saleh, J. Hazard. Mater. **185**, 17–23 (2011)

9. M. Sathishkumar, A.R. Binupriya, D. Kavitha, R. Selvakumar, R. Jayabalan, J.G. Choi, S.E. Yun, Chem. Eng. J. **147**, 265–271 (2009)
10. E. Bilgin Simsek, B. Aytas, D. Duranoglu, U. Beker, A.W. Trochimczuk, Desalt. Water Treat. **57**, 1–17 (2015)
11. J.P. Wang, H.M. Feng, H.Q. Yu, J. Hazard. Mater. **144**, 200–207 (2007)
12. Q.-S. Liu, T. Zheng, P. Wang, J.-P. Jiang, N. Li, Chem. Eng. J. **157**, 348–356 (2010)
13. X. Li, S. Chen, X. Fan, X. Quan, F. Tan, Y. Zhang, J. Gao, J. Colloid Interface Sci. **447**, 120–127 (2015)
14. Q. Lu, G.A. Sorial, J. Hazard. Mater. **167**, 89–96 (2009)
15. H. Ding, X. Li, J. Wang, X. Zhang, C. Chen, J. Environ. Sci. **43**, 187–198 (2016)
16. J. Xu, T. Sheng, Y. Hu, S.A. Baig, X. Lv, X. Xu, Chem. Eng. J. **219**, 162–173 (2013)
17. M.A. Salam, M. Mokhtar, S.N. Basahel, S.A. Al-Thabaiti, A.Y. Obaid, J. Alloys Compd. **500**, 87–92 (2010)
18. C. Wang, R. Ma, Q. Wu, M. Sun, Z. Wang, J. Chromatogr. A **1361**, 60–66 (2014)
19. T.A. Saleh, V.K. Gupta, Adv. Colloid Interface Sci. **211**, 93–101 (2014)
20. V.K. Gupta, R. Kumar, A. Nayak, T.A. Saleh, M.A. Barakat, Adv. Colloid Interface Sci. **193–194**, 24–34 (2013)
21. F. Helfferich, *Ion Exchange* (Dover, New York, 1995)
22. P. Kirkegaard, M. Eldrup, O.E. Mogensen, N.J. Pedersen, Comput. Phys. Commun. **23**, 307–335 (1981)
23. K.S. Liao, H. Chen, S. Awad, J.-P. Yuan, W.-S. Hung, K.-R. Lee, J.-Y. Lai, C.-C. Hu, Y.C. Jean, Macromolecules **44**, 6818–6826 (2011)
24. S. Biniak, M. Pakula, A. Swiatkowski, K. Kusmierek, G. Trykowski, React. Kinet. Mech. Catal. **114**, 369–383 (2014)
25. J. Zhang, J. Lei, H. Ju, C. Wang, Anal. Chim. Acta **786**, 16–21 (2013)
26. R. Hoseinzadeh Hesas, A. Arami-Niyaa, W.M.A. Wan Dauda, J.N. Sahu, J. Anal. Appl. Pyrol. **104**, 176–184 (2013)
27. A. Sharma, B.K. Lee, J. Environ. Manag. **165**, 1–10 (2016)
28. X. Li, W. Wang, J. Dou, J. Gao, S. Chen, Z. Quan, H. Zhao, J. Water. Process. Eng. **9**, e14–e20 (2016)
29. J. Bandara, J.A. Mielczarski, J. Kiwi, Appl. Catal. B Environ. **34**, 307–320 (2001)
30. B. Yang, Y. Liu, Z. Li, L. Lei, J. Zhou, Z. Zhang, Environ. Sci. Pollut. Res. **23**, 1482–1491 (2016)
31. H. Yuh-Shan, Scientometrics **59**, 171–177 (2004)
32. Y.S. Ho, G. McKay, Process Biochem. **34**, 451–465 (1999)
33. J. Fan, J. Zhang, C. Zhang, L. Ren, Q. Shi, Desalination **267**, 139–146 (2011)
34. C. Namasivayam, D. Kavitha, J. Hazard. Mater. **B98**, 257–274 (2003)
35. O. Aktas, F. Cecen, J. Hazard. Mater. **141**, 769–777 (2007)
36. I.A.W. Tan, A.L. Ahmad, B.H. Hameed, J. Hazard. Mater. **164**, 473–482 (2009)
37. B. Özkaya, J. Hazard. Mater. **B129**, 158–163 (2006)
38. M. Radhika, K. Palanivelu, J. Hazard. Mater. **B138**, 116–124 (2006)
39. F. Salvador, N. Martin-Sanchez, R. Sanchez-Hernandez, M.J. Sanchez-Montero, C. Izquierdo, Microporous Mesoporous Mater. **202**, 277–296 (2015)